

See discussions, stats, and author profiles for this publication at: <https://www.researchgate.net/publication/234875300>

Microscopic equations of state of polyethylene: Hard-chain contribution to the pressure

ARTICLE *in* THE JOURNAL OF CHEMICAL PHYSICS · JANUARY 1993

Impact Factor: 2.95 · DOI: 10.1063/1.464280

CITATIONS

47

READS

5

4 AUTHORS, INCLUDING:



John McCoy

New Mexico Institute of Mining and Tech...

114 PUBLICATIONS 2,055 CITATIONS

SEE PROFILE

Microscopic equations of state of polyethylene: Hard-chain contribution to the pressure

Arun Yethiraj

Department of Materials Science and Engineering and Materials Research Laboratory, University of Illinois, 1304 West Green Street, Urbana, Illinois 61801

John G. Curro

Sandia National Laboratories, Albuquerque, New Mexico 87185

Kenneth S. Schweizer

Department of Materials Science and Engineering and Materials Research Laboratory, University of Illinois, 1304 West Green Street, Urbana, Illinois 61801

John D. McCoy

Materials and Metallurgical Engineering Department, New Mexico Institute of Mining and Technology, Socorro, New Mexico 87801

(Received 17 August 1992; accepted 30 September 1992)

The athermal contribution to the pressure of polyethylene is investigated via integral equations and mean field generalized Flory-type theories. The molecules are modeled as fused-hard-sphere chains with fixed bond lengths and bond angles; torsional rotations are treated via the rotational isomeric state approximation with literature values for the *trans-gauche* energies. The hard sphere diameter is obtained by matching structure factor predictions of the polymer reference interaction site model (PRISM) theory for hard chains to data from wide-angle scattering experiments. In all, five hard chain equations of state are investigated: three via different thermodynamic routes in the PRISM theory, and two via different extensions (to fused-sphere chains) of the generalized Flory-dimer (GFD) theory. The integral equation approaches consist of a free energy "charging" route, the compressibility route, and the "wall" route (where the pressure is obtained from the density profile of the fluid at a hard wall). The two GFD approaches correspond to different choices for the reference monomer and dimer fluids required in the theory. Each of the five equations of state results in significantly different predictions for the pressure. The predictions of the various equations relative to each other are nearly independent of chain length, and this allows us to draw conclusions for polymeric fluids (where simulation results are not available) by testing the performance of the equations for diatomics (where simulation results are available). We thus speculate that the charging route overestimates the pressure, the compressibility route underestimates the pressure, and the GFD and wall equations of state are the most accurate.

I. INTRODUCTION

Empirical equations of state that contain adjustable parameters are widely used in industry to obtain the thermodynamic properties of alkanes.¹ While such an approach is definitely useful, the use of empirical equations of state is accompanied by three major disadvantages: (i) a large amount of experimental data is required in order to fit the parameters in the equations of state; (ii) the equations of state are not very accurate outside the range where their parameters have been fit to data; and (iii) the parameters in the equation of state often have little physical meaning. An equation of state that has a sound theoretical basis is expected to rectify these deficiencies.

Several equation of state theories for chain-molecule fluids have been reported in the literature. Most of these theories are based either on a lattice model of the polymer,² or on the *c* parameter theory of Prigogine³ (which relates the chain-fluid entropy to the hard sphere entropy via an empirical *c* parameter). All these theories contain adjustable parameters which are determined by fitting to exper-

iment. Although the parameters in the lattice-based equations have more meaning than those in purely empirical equations, the physical insight they offer is clouded by several qualitative concepts such as free volume.

There has been considerable effort to obtain a more thorough understanding of chain-molecule fluids both via theory⁴⁻⁸ and computer simulation.^{7,9,10} Computer simulations have been performed on realistic models of alkanes.^{9,10} Since they are exact for a given model, they permit a direct evaluation of the ability of a model to mimic the real fluid. Simulations are computationally intensive, however, and thus far have been restricted to fairly short chains. Theoretical effort has concentrated on simple models for chain molecules such as the freely jointed hard chain^{4,5,8,11} and the square-well chain model.^{6,7} These models provide a starting point for the study of chain-molecule fluids; once these models are understood more realistic interactions may be incorporated.

We are interested in obtaining microscopic equations of state for alkanes, especially polyethylene (PE). The phi-

losophy of our approach is to start with a realistic molecular model for the alkane molecules, and then use current methods of statistical mechanics to obtain the volumetric properties. The parameters in the molecular model, i.e., the intermolecular potentials, may be, in principle, estimated independently of the equation of state data we aim to describe. This procedure should give an equation of state that contains no adjustable parameters.

The hydrocarbon molecules are modeled as a chain of (identical) "interaction sites." The intermolecular potential between two molecules is the sum of site-site interactions; a site-site Lennard-Jones intermolecular potential is employed. The bond lengths and bond angles in each molecule are fixed; torsional rotations are treated via the rotational isomeric state (RIS) approximation.

First order Barker-Henderson (BH) perturbation theory¹² on the free energy appears to be a promising route to obtaining the thermodynamic properties of polymers. In this approach, the site-site intermolecular potential is divided into a repulsive part and an attractive part; the repulsive part of the potential is then replaced with a hard sphere (reference) potential. The free energy of the real system is then expressed as a sum of the reference free energy and a perturbation free energy due to the attractions. Differentiation of the free energy gives the pressure. Implementation of this method requires two quantities: the free energy (or equation of state) of the reference system, and the local structure of the reference system. The BH approach has been shown to be accurate for the equation of state of (short) square-well chains when compared to simulations,⁷ and it is therefore of interest to implement it for realistic models of polymers. In this paper, we focus on the equation of state of the reference (hard chain) system. A future publication will describe the perturbation theory and comparison with experiment.¹³

The objective of this paper is to obtain equations of state for hard-chain models with some degree of chemical realism in terms of bond lengths, bond angles, etc. Most of the hard chain equations of state mentioned earlier,⁸ with the exception of the generalized Flory theories,^{4,5} cannot be extended to such models. Here we apply the generalized Flory-dimer (GFD) theory⁵ to the fused-sphere RIS model of alkanes. We motivate that the GFD theory for alkanes is not unique; in addition to the equation proposed by Honnell and Hall,⁵ we present a different equation of state obtained via a different choice of the reference monomer and dimer fluids required in the theory.

We investigate various routes to the hard-chain pressure using the polymer reference interaction site model (PRISM) integral equation theory of Curro and Schweizer.¹⁴ The PRISM theory is a generalization to polymers of the small-molecule RISM theory of Chandler and co-workers.¹⁵⁻¹⁷ For homopolymer fluids, Curro and Schweizer^{14,18} reduce the order N^2 (N is the number of sites per molecule or the chain length in a linear polymer) coupled nonlinear equations in the RISM theory to a single nonlinear equation by neglecting explicit chain end effects. The PRISM theory has been shown to be very accurate for the intermolecular distribution function when compared to

Monte Carlo simulations of hard chains^{19,20} and molecular dynamics simulations of repulsive Lennard-Jones chains.²¹ It has also been successful in predicting the structure factor in alkane and polyethylene melts,²² and provides the crucial liquid phase information in a recent first principles density functional theory of chain molecule crystallization.²³

One of the appealing features of the PRISM theory is that it allows the study of chemically realistic models of polymers. Furthermore, since PRISM is a theory for fluid structure, predictions for the structure factor may be directly compared to scattering experiments thereby allowing one to estimate potential parameters in the model independently of the predictions for the thermodynamics. This is how the hard-sphere diameter for the model alkanes will be obtained.

The PRISM theory, like most integral equation theories for simple fluids, is not without some disadvantages. For one, the calculation of the pressure depends on which thermodynamic route is used. Also, the theory is expected to be more accurate for the short wavelength properties of the fluid.¹⁷ Another difficulty is that since the virial pressure in a polymer is a function of three-body correlations in the fluid,²⁴ PRISM (which provides only pair correlations) must be supplemented with some approximation to the three-body correlations if the virial pressure is desired.

Schweizer and Curro¹¹ have used PRISM to study the equation of state of fully flexible tangent-sphere hard chains. The pressure was calculated via the compressibility equation, and the virial theorem with a superposition approximation for the three-body correlations. The theories were in good agreement with simulations for short chains, but the accuracy deteriorates with increasing chain length. It has since been shown^{19,25} that the superposition approximation employed in Ref. 11 is not very accurate. The virial route therefore does not appear to be promising and will not be considered in this work.

We investigate three alternatives for the hard chain contribution to the pressure via the PRISM theory. Two equations of state are obtained by solving PRISM for a bulk polymer fluid, and calculating the pressure via the compressibility equation, and a free energy charging (or coupling parameter) technique, respectively. The compressibility equation relates the pressure to an integral of the zero wave vector component of the structure factor; the coupling parameter technique estimates the free energy change due to the inflating of the hard spheres from points to full size. A third equation of state is obtained via the extension of the PRISM theory to nonuniform polymers done by Yethiraj and Hall.²⁶ In this case the integral equation is solved for a polymeric fluid at a hard wall; the pressure is simply related to the density of chain sites at the hard wall.²⁷

We find that all five equations of state give different results for the pressure. Since computer simulations of athermal alkanes are not available, it is not possible to determine unambiguously which of the equations of state is the most accurate. However, we find that the relative behavior of the various equations of state is not a strong

function of chain length. Therefore, from a comparison of the theories to simulations for diatomics we conclude that one of the GFD extensions, and the predictions using the wall method, are the most accurate. The charging route significantly overestimates the pressure, and the compressibility route significantly underestimates the pressure (when compared to the GFD and wall routes).

The remainder of this paper is organized as follows: in Sec. II we describe the molecular model and the estimation of the hard sphere diameters; in Sec. III we describe the PRISM theory and the various thermodynamic routes to the pressure; in Sec. IV the GFD theory and its extension to fused-sphere chains is presented; in Sec. V we present and discuss results for the structure and thermodynamics; and in Sec. VI we present our conclusions.

II. MOLECULAR MODEL

A. Intramolecular interactions

We employ the standard rotational isomeric state (RIS) model²⁸ for the chain molecules. In this model, one makes the approximation that the (long-range) excluded volume interactions between two sites on a single molecule are effectively screened out (the ideality hypothesis²⁹) and describe single chain properties via a model that includes only local interactions.

Each molecule is modeled as a chain of fused-hard spheres of diameter, d . The bond length, l , and the bond angle, θ , are constrained to be fixed at their average equilibrium values. Torsional rotations are constrained to three discrete angles: the *trans*, the *gauche*⁺, and the *gauche*[−]; the *gauche* conformations are located at $\pm 120^\circ$ relative to the *trans*. The intramolecular potential energy is completely determined by the energies associated with the torsional rotations. The *trans*–*gauche* energies are fixed at 500 cal/mol for polyethylene, and 700 cal/mol for butane. Successive *gauche*⁺/*gauche*[−] combinations are given an additional 2000 cal/mol to account for the “pentane” effect.²⁸ For butane, we use the continuous rotational potential employed by Ryckaert and Bellemans³⁰ in the calculation of the single chain structure factor. The results obtained using this potential are indistinguishable from those obtained using the RIS potential with a *trans*–*gauche* energy of 700 cal/mol.

B. Intermolecular interactions

A Lennard-Jones (LJ) potential is expected to be sufficient to model the interaction between sites on different molecules. It is not easy, however, to estimate the potential parameters. One way to determine the LJ parameters is via a comparison of computer simulations to experiments. In this method the potential parameters employed in the simulations are adjusted in order to reproduce some experimental thermodynamic property, such as the internal energy or the second virial coefficient. The earliest such estimation of LJ parameters for the alkanes is probably due to Ryckaert and Bellemans³⁰ via simulations for the internal energy. More recently, Lopez Rodriguez *et al.*³¹ have done a very thorough study of LJ parameters for the lower

alkanes via calculations of the second virial coefficient. In their treatment they allowed different LJ well depths between the CH₃–CH₃, CH₂–CH₂, and CH₂–CH₃ moieties. There are two problems associated with the above approaches: (i) it is not possible to obtain *independent* estimates for *both* the well depth *and* the collision diameter, and (ii) the potential parameters seem to depend on which thermodynamic property is matched to the corresponding experimental value. For example, Lopez Rodriguez *et al.*³¹ and Ryckaert–Bellemans³⁰ report very different numbers for the LJ well depth in alkanes.

Given a theory for the microscopic correlations in the fluid, it might be possible to extract the LJ parameters by “inverting” experimental structure factor measurements. This program has been carried out with some success for simple fluids³² and for diatomic molecules,³³ and could possibly be extended to polymers via the PRISM theory. We do not attempt this approach here, however, because the accuracy of PRISM for fluids interacting via the LJ potential is not known³⁴ and this introduces considerable uncertainty into the method. We do, however, estimate an effective hard-core diameter (PRISM is known to be accurate for hard chains²⁰) via comparison of theory to experiments for the total structure factor. In a future publication,¹³ we will make use of this result to estimate the full LJ potential for alkanes.

In this paper, we focus on the athermal contribution to the pressure by employing a hard-core model for the site-site intermolecular potential. The philosophy is to add in the attractive contribution as a perturbation to the athermal contribution. The hard-sphere diameter, d , is obtained via a comparison of the total structure factor from the PRISM theory to x-ray diffraction data.²² The hard-sphere diameter used in the theory is adjusted until the first peak in the structure factor matches the experimentally measured value.²² Since the first peak in the structure factor reflects primarily local interchain packing which is dominated by the hard-core part of the potential, we expect that this method will give an accurate estimate for d . Figure 1 compares the theoretical prediction for the structure factor (using $d=3.9$ Å, which was determined by trial and error) to x-ray diffraction data.²² The agreement between theory and experiment is very good over the entire experimental range, except perhaps at small k .³⁵ The agreement between theory and experiment in Fig. 1 gives us confidence in the estimation of d as well as in the approximate evaluation of the intramolecular structure factor. The value for the hard-sphere diameter of polyethylene (3.9 Å) obtained above is reasonable and consistent with solid geometrical calculations based on atomic radii and bond lengths of Slonimskii *et al.*³⁶ The hard-sphere diameter of butane at 300 K is estimated in a similar manner to be 3.77 Å.³⁷ Note that these hard-sphere diameters will be dependent on both temperature and chain length. The latter feature appears to reflect the small errors incurred by collapsing the hydrogen atoms onto the carbon center which thereby ignores interlocking of CH₂ groups on different chains at high densities.³⁷ The potential parameters are summarized in Table I.

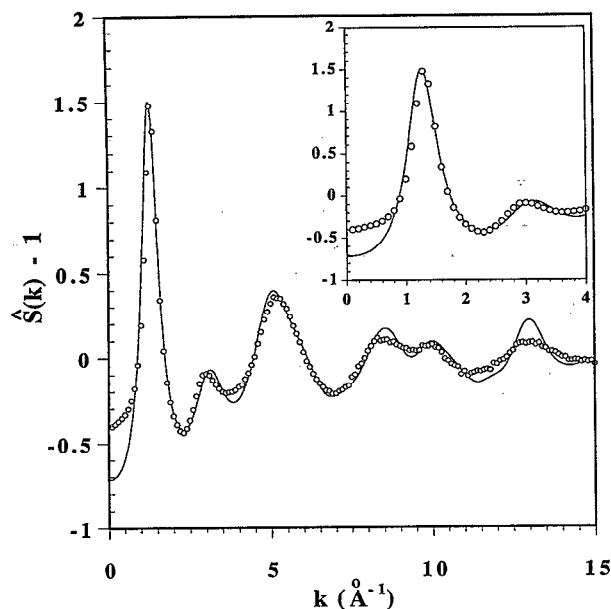


FIG. 1. Comparison of experimental data for the structure factor of polyethylene ($N=6429$) at 430 K (O) to PRISM predictions using a hard-sphere diameter of $d=3.9$ Å (Ref. 22). The inset shows the amorphous halo region. The reader is referred to Ref. 22 for a complete discussion of this comparison.

III. POLYMER-RISM THEORY

A. Polymer-RISM theory for bulk polymers

The polymer-RISM equation^{14,18} relates the average site-site total correlation function, $h(r)[\equiv g(r)-1]$, to the average site-site direct correlation function, $c(r)$, and the intramolecular distribution function, $\omega(r)$, via a nonlinear integral equation which may be written (in Fourier space) as

$$\hat{h}(k) = \hat{\omega}(k) \hat{c}(k) \hat{\omega}(k) + \rho_m \hat{\omega}(k) \hat{c}(k) \hat{h}(k), \quad (1)$$

where the carets denote Fourier transforms, i.e.,

$$\hat{f}(k) = \frac{4\pi}{k} \int_0^\infty r f(r) \sin(kr) dr, \quad (2)$$

ρ_m is the monomer (or segmental) density of the chain fluid ($\rho_m = N\rho$, where N is the degree of polymerization and ρ is the number density of chains),

$$g(r) = \frac{1}{N^2} \sum_{i,j} g_{ij}(r), \quad (3)$$

TABLE I. Potential parameters for butane and polyethylene (PE). The hard-sphere diameters are estimated from the scattering data at 300 K for butane and at 430 K for polyethylene.

| | d (Å) | l (Å) | θ (deg) |
|--------|---------|---------|----------------|
| Butane | 3.77 | 1.53 | 109.47 |
| PE | 3.90 | 1.54 | 112.00 |

$$\omega(r) = \frac{1}{N} \sum_{i,j} \omega_{ij}(r), \quad (4)$$

$g_{ij}(r)$ is related to the probability that sites i and j on different chains are a distance r apart, and $\omega_{ij}(r)$ is the probability that sites i and j on the same chain are a distance r apart. The function $c(r)$ is defined implicitly through Eq. (1).

Given an expression for the intramolecular correlation function $\omega(r)$ and a closure relation between $h(r)$ and $c(r)$, the polymer-RISM equation may be solved to obtain $h(r)$ and $c(r)$, and therefore $g(r)$. In general, since the functions $h(r)$ and $c(r)$ are functionals of $\omega(r)$ (and vice versa), they should be determined in a self-consistent manner; the self-consistency problem has recently been addressed.³⁸ In polymer melts, however, the Flory ideality hypothesis²⁹ allows for a considerable zeroth order simplification of the problem. Within the ideality approximation one may calculate $\omega(r)$ from a single chain model which ignores long-range repulsions and many body medium-induced interactions. This is the approach we employ in this work.

The single chain structure factor for the rotational isomeric state chain (without excluded volume) is calculated exactly for sites separated by five or less bonds, and approximately using the discrete Koyama distribution for segments separated by more than five bonds. The calculation of $\hat{\omega}(k)$ is identical to that described in Ref. 39, and the reader is referred to that paper for details. Comparisons with Monte Carlo simulations have shown that this computationally convenient approximation is very accurate.³⁹

The polymer-RISM equation relates one unknown function, $h(r)$, to another unknown function, $c(r)$. In order to solve this equation another ("closure") relation between $h(r)$, $c(r)$, $\omega(r)$, and the intermolecular potential is required. For the hard-chain model considered in this paper, the exact hard-core condition gives

$$h(r) = -1, \quad r < d. \quad (5)$$

Another (approximate) relation between $h(r)$ and $c(r)$ outside the core is generally obtained from analogy with integral equation theories for simple (atomic) fluids.

By analogy with the Percus-Yevick (PY) theory of simple hard-sphere fluids, and the RISM theory of molecular fluids,¹⁷ Curro and Schweizer^{14,18} suggested

$$c(r) = 0, \quad r > d. \quad (6)$$

The polymer-RISM theory with the PY closure has been shown to be quite accurate for both the local and long range ("correlation hole") structure of hard chains,^{19,20,40} repulsive Lennard-Jones chains,²¹ and polyethylene melts.²² Alternative closure approximations for hard chains have recently been investigated, and the PY closure appears to be the most accurate.⁴⁰

B. Structure factor and thermodynamic properties

In the PRISM theory, the structure factor, $\hat{S}(k, \rho_m)$, is given by

$$\hat{S}(k, \rho_m) = \frac{\hat{\omega}(k)}{1 - \rho_m \hat{\omega}(k) \hat{c}(k)}. \quad (7)$$

The equation of state may be calculated from the zero wave vector component of the structure factor using the compressibility equation¹¹

$$\beta P = \int_0^{\rho_m} d\rho'_m \hat{S}^{-1}(0, \rho'_m), \quad (8)$$

where $\beta = 1/k_B T$, k_B is Boltzmann's constant, T is the temperature, and P is the pressure. We will refer to Eq. (8) as the "compressibility route" to the pressure. Since the pressure is obtained via an integration of the compressibility from zero density to the density of interest, this route may incur significant errors for polymers, since (i) the ideality hypothesis employed in the theory is not accurate at low densities, and (ii) PRISM theory is known to be less accurate at low densities than it is at meltlike densities even when $\hat{\omega}(k)$ is known exactly.^{19,20} The latter is true even of the RISM theory for small-molecule fluids.¹⁷ Therefore, it is of interest to investigate other thermodynamic routes to the equation of state.

In earlier work, two of us (K.S.S. and J.G.C.) investigated a virial route to the equation of state.¹¹ For polymers, the virial equation may be written as^{11,24}

$$\frac{\beta P}{\rho} = 1 + \frac{2\pi}{3} N \rho_m d^3 g(d^+) + R_3, \quad (9)$$

where R_3 is a density-dependent quantity that depends on three-body correlations in the fluid. Since three-body correlations are difficult to calculate, a physically plausible superposition approximation was invoked to evaluate R_3 from the intramolecular and intermolecular pair correlation functions. A comparison with Monte Carlo simulations showed that this theory underestimated the pressure, in a way which appears to significantly worsen with increasing chain length. It has since been shown that the superposition approximation is not very accurate for R_3 .^{19,25} Therefore, we do not investigate this route to the pressure any further.

An alternative route to the equation of state has been proposed by Lowden and Chandler.^{17,41} They used a functional integration procedure (similar to the coupling parameter approach commonly used in statistical mechanics⁴²) to obtain the change in the free energy of the fluid due to the "inflating" of the (polyatomic) molecules from point masses (of zero diameter) to hard-core molecules. (The bond length remains the same throughout). The generalization to polymers is immediate, and the resulting expression for homopolymers is

$$\beta \frac{A - A_0}{V} = 2\pi \rho_m^2 d^3 \int_0^1 d\lambda \lambda^2 g^{(\lambda)}(\lambda d^+), \quad (10)$$

where A is the free energy of the hard-core fluid, A_0 is the free energy of a fluid of noninteracting (ideal) polymer molecules, and $g^{(\lambda)}(\lambda d^+)$ is the contact value of $g(r)$ for a hard-core polymer fluid whose molecules have a site diameter of λd . The pressure is then obtained by a (numerical) differentiation of the free energy. For monatomic fluids Eq.

(10) reduces to the usual virial equation. We refer to Eq. (10) as the "charging" route to the equation of state.

C. Wall polymer-RISM Theory

An equation of state for bulk polymeric fluids may be obtained from the density profile of the fluid at a hard wall.²⁷ If the hard wall (impenetrable to the centers of chain sites) is located at $z=0$, and $\rho(z)$ is the density profile of the fluid at this wall, then the "wall sum rule" states that²⁷

$$\beta P = N \rho(0). \quad (11)$$

We employ the theory of Yethiraj and Hall for polymer fluids at a wall,²⁶ to calculate the pressure of the bulk polymer. This provides an alternative route to the equation of state which is different from those discussed earlier.

The wall-polymer-RISM theory²⁶ is a generalization to polymers of the theories of Henderson *et al.*⁴³ for the adsorption of hard spheres at a wall, and of Zhou and Stell⁴⁴ for the adsorption of hard spheres between two walls. This approach combines the polymer-RISM theory and the growing adsorbent model⁴³ to obtain the density profile of the fluid at a hard wall. The starting point in the theory is the set of polymer-RISM equations for a binary mixture of hard spheres and polymers. The hard spheres are then made infinitely dilute and infinitely large (in that order). In this limit, the hard sphere becomes a wall, and one can calculate the density profile of the polymer fluid at the wall from the wall-fluid correlation function. When the ideality hypothesis is invoked in order to calculate the single chain structure factor, the bulk fluid correlation functions rigorously decouple from the wall-fluid correlations, allowing one to calculate them independently. Once the bulk correlation functions have been obtained [using Eq. (1) with the PY closure], the wall-fluid correlation function, $g_w(z)$, can be calculated from the wall polymer-RISM equation,²⁶

$$\tilde{g}_w(k) = \hat{S}(k, \rho_m) \tilde{C}_p(k) \quad (12)$$

where $C_p(z)$ is the wall-fluid direct correlation function, and

$$\tilde{f}(k) = \int_{-\infty}^{\infty} f(z) \exp(ikz) dz. \quad (13)$$

For hard chains at a hard wall the PY closure relations are,²⁶

$$g_w(z) = 0, \quad z < 0, \quad (14)$$

$$C_p(z) = \hat{S}^{-1}(0, \rho_m), \quad z > 0. \quad (15)$$

For numerical convenience, Eq. (12) is actually solved for a fluid confined between two walls at a separation H ; the single wall case is recovered in the limit as H becomes large. For all the cases studied in this work, we find that the large H limit is reached well before $H \approx 20 d$. The calculations presented in this work employ a value of $H = 40 d$.

The pressure is calculated from the wall sum rule, which may be written as

$$\frac{Z}{N} \frac{\beta P}{\rho_m} = g_w(0). \quad (16)$$

This theory is known to be poor at low densities;²⁶ in fact it *does not* satisfy the ideal gas condition: $Z \rightarrow 1$ as $\rho \rightarrow 0$. However, it has been shown to be accurate for the density profiles (and hence the pressure) at moderate and high densities.²⁶

IV. GENERALIZED FLORY-DIMER (GFD) THEORY

The GFD theory of Honnell and Hall,⁵ which is based on the Dickman–Hall generalized Flory theory,⁴ relates the pressure of a fluid composed of hard chains to those of a fluid composed of hard spheres and a fluid composed of hard dimers. Originally derived for freely jointed hard-sphere chains, it has since been extended to athermal star polymers⁴⁵ and square-well chains.⁶ A comparison between the GFD theory and computer simulations of hard chains,^{25,27} star polymers,⁴⁵ and square-well chains⁷ has shown that the theory is excellent for the pressure of chain fluids for a wide range of chain lengths, densities, and temperatures. The success of the GFD theory in describing these model chain fluids motivates its application to the investigation of the properties of real alkanes.

In this section we investigate extensions of the GFD theory to treat fluids composed of fused hard-sphere chains, and calculate the hard-sphere contribution to the pressure in butane and polyethylene. In what follows we first briefly describe the GFD theory for tangent sphere chains, and then outline two ways in which the theory can be extended to treat fused sphere chains.

A. GFD theory for tangent hard-sphere chains

In the GFD theory, the probability of inserting a single chain into a chain fluid is estimated from that of inserting a monomer into a monomer fluid and that of inserting a dimer into a dimer fluid. From this information, a simple equation of state for chain molecule fluids is obtained, which is given by

$$Z(N, \eta) = (1 + Y_N)Z(2, \eta) - Y_N Z(1, \eta), \quad (17)$$

where $Z(i, \eta)$ is the compressibility factor ($\equiv \beta P / \rho$) of an i -mer fluid at packing fraction, η ($\equiv v_0 d^3 \rho$, where $v_0 d^3$ is the volume of a single chain molecule), and Y_N is given by

$$Y_N = \frac{v_e(N) - v_e(2)}{v_e(2) - v_e(1)}, \quad (18)$$

where $v_e(i)$ is the volume excluded by an i -mer to a monomer averaged over all conformations of the i -mer. The excluded volume is an estimate of the amount of space required for the insertion of the chain molecule. Equation (17) is the GFD equation of state. The quantities $Z(1, \eta)$ and $Z(2, \eta)$ are assumed to be known; in their work Honnell and Hall⁵ use the Carnahan–Starling⁴⁶ and the Tildesley–Streett⁴⁷ equations, respectively.

B. Extension to fused sphere chains

The extension of the GFD theory to fused-sphere chains is straightforward, but not unique. Consider a fused-sphere chain consisting of N hard spheres of diameter d that are joined together with bond lengths of l . Implementation of the GFD theory for this fluid consists of two steps: identifying the monomer and dimer fluids whose compressibility factors appear in Eq. (17), and calculating the required excluded volumes and monomer and dimer pressures. Once the appropriate monomer and dimer fluids in Eq. (17) have been identified, implementation of the GFD theory is straightforward.

For fused-sphere chains, the identification of the appropriate monomer and dimer fluids is not obvious. If one were to simply relax all the bonding constraints in the molecules of the chain fluid to obtain the monomer fluid, then the total packing fraction of the system would increase (since previously overlapping spheres cannot do so anymore) if the site density of the system is kept constant. The same is true if one were to simply snip every second bond in the molecules of the chain fluid in order to obtain the dimer fluid. On the other hand, if one were to force the packing fraction of the monomer and dimer fluids to be the same as in the chain fluid (keeping d and l in these fluids to be the same as in the chain fluid) the site density of the monomer and dimer fluids would be different from the chain fluid. Another option is to choose both the packing fraction and site density of the monomer (and dimer) fluids to be the same as in the chain fluid, but allow the hard-sphere diameters of the monomers (and dimers) to change.

The first route we investigate is the one proposed by Honnell and Hall in their study of rigid triatomics,⁵ i.e., we assume that the diameters of the monomers and dimers are the same as in the chain fluid and evaluate the monomer and dimer pressures at the same packing fraction as the chain fluid by adjusting the site fraction. We call the equation of state thus obtained GFD-A, to distinguish it from the other approach described below.

Physically, we believe it is more appropriate to allow the diameters of the monomers and dimers to change. One can visualize the monomer fluid as being formed from a crude cutting up of the N -mer into N pieces. Taken literally, for our model, this would result in a fluid of spheres with spherical caps missing. Since equations of state for these molecules are difficult to obtain and not available in the literature, one could replace each of the molecules with a hard sphere. This is what we do in this work. We then choose the *effective* diameter of this hard sphere by requiring that the volume of N such spheres be the same as that of a single chain molecule. Similarly the chain is cut up into $N/2$ pieces, each of which is then replaced by a hard dimer with the same bond length as in the chain molecules but with an *effective* hard-sphere diameter that is different from that of the spheres composing the chain molecule. Identifying the monomer and dimer fluids then reduces to calculating the effective hard sphere diameters of the monomers and the dimers (which will be different in general). We call the equation of state thus obtained GFD-B.

The effective hard-sphere diameters of the monomer (denoted d_m) and the dimer (denoted d_d) in the GFD-B theory are readily calculated by equating the volumes of N monomers and $N/2$ dimers to that of a single chain molecule. (Note that $d_m = d_d = d$ in the GFD-A theory.) If the volume of a single chain molecule is $v_0 d^3$, then

$$N \frac{\pi d_m^3}{6} = v_0 d^3 \quad (19)$$

and

$$\left(\frac{N}{2}\right) \frac{\pi}{6} d_d^3 \left[1 + \frac{3}{2} \left(\frac{l}{d_d}\right) - \frac{1}{2} \left(\frac{l}{d_d}\right)^3\right] = v_0 d^3. \quad (20)$$

C. Equations of state for monomers and dimers

The monomer and dimer compressibility factors are obtained from the (essentially exact) Carnahan–Starling⁴⁶ and Tildesley–Streett⁴⁷ equations of state, respectively. The Carnahan–Starling⁴⁶ equation of state for hard spheres is given by

$$Z(1, \eta) = \frac{1 + \eta + \eta^2 - \eta^3}{(1 - \eta)^3}, \quad (21)$$

and the Tildesley–Streett⁴⁷ equation of state for hard diatomics is given by

$$Z(2, \eta) = \frac{1 + F\eta + G\eta^2 - H\eta^3}{(1 - \eta)^3}, \quad (22)$$

where

$$F = 1 + 0.378\,36x + 1.0786x^3, \quad (23)$$

$$G = 1 + 1.303\,76x + 1.8001x^3, \quad (24)$$

$$H = 1 + 2.398\,03x + 0.3570x^3, \quad (25)$$

and x is the ratio of the bond length to the hard sphere diameter ($x \equiv l/d_d$).

D. Evaluation of excluded volumes

The excluded volumes of the monomer and dimer can be calculated exactly, and are given by

$$v_e(1) = \frac{4\pi}{3} d_m^3 \quad (26)$$

and

$$v_e(2) = \frac{\pi}{6} (d_m + d_d)^3 \left[1 + \frac{3}{2} \left(\frac{l}{d_m + d_d}\right) - \frac{1}{2} \left(\frac{l}{d_m + d_d}\right)^3\right], \quad (27)$$

respectively.

The N -mer excluded volume averaged over all chain conformations cannot be evaluated exactly, and we resort to a Monte Carlo simulation method similar to that described in Refs. 45 and 48. Random conformations of the chain molecules are placed in the center of a box. A monomer (of diameter d_m) is placed successively at many randomly chosen points in the box and checked for overlap

TABLE II. Volume and excluded volume for butane. The columns titled A and B refer to calculations that use $d_m = d$, and d_m given by Eq. (19), respectively. In these calculations $N = 4$, and $l = 1.53$ Å.

| d (Å) | T (K) | $v_0/(Nd^3)$ | $v_e(N)/(Nd^3)$ | | Y_N/N | |
|---------|---------|--------------|-----------------|-------|---------|--------|
| | | | A | B | A | B |
| 3.668 | 291.5 | 0.352 | 1.861 | 1.596 | 0.3802 | 0.3979 |
| 3.717 | 199.9 | 0.351 | 1.877 | 1.606 | 0.4012 | 0.4095 |
| 3.6939 | 274.0 | 0.351 | 1.860 | 1.593 | 0.3835 | 0.3998 |
| 3.77 | 300.0 | 0.348 | 1.839 | 1.570 | 0.3796 | 0.3952 |

with the chain molecule. The excluded volume of each conformation is given by

$$v_e = \frac{N_0}{N_p} V, \quad (28)$$

where N_0 is the number of monomer positions that result in an overlap, N_p is the number of monomer positions attempted, and V is the volume of the box. Errors in these calculations are about 1%.

The method described above is first used to calculate the volume of the molecule $v_0 d^3$. This is done by choosing a trial monomer of zero size in the simulation procedure. Once v_0 is known, we proceed with the calculation of the excluded volumes. The excluded volumes required for the two versions of the GFD theory (GFD-A and GFD-B) are calculated simultaneously, using both $d_m = d$ and the d_m given by Eq. (19).

For butane, within the RIS model, there are only three independent conformations, and the excluded volume of each of these is obtained via the above method using $N_p = 10^7$. The average excluded volume, $v_e(N)$, is calculated by weighting the excluded volume of each of the individual conformations by the statistical weight of that conformation. The process is repeated five times in order to obtain statistical uncertainties in the calculation. Results for the volume and excluded volume of the butane models considered are given in Table II. As expected the excluded volume for GFD-A is higher than that for GFD-B (since d_m is larger). However, the parameter Y_N is actually smaller in the GFD-A theory than it is in the GFD-B theory. This is because $v_e(2) - v_e(1)$ (which appears in the denominator of the expression for Y_N) is also larger in the GFD-A theory. Since both Y_N and the dimer bond length to diameter ratio are smaller in the GFD-A theory, the GFD-A theory will always predict lower pressures than the GFD-B theory for butane.

An approximate evaluation of $v_e(N)$ for polyethylene may be carried out by noting that, for large N , $\Delta v_e(N) \equiv v_e(N) - v_e(N-1)$ becomes independent of N .⁴ In fact, applications of the GF-type theory to tangent sphere models⁴⁻⁶ have all employed the approximation $\Delta v_e(N) \approx \Delta v_e(3)$ (which can be calculated exactly) for $N > 3$. For the fused sphere case we estimate $\Delta v_e(N)$ from simulations for chains of length $n = 14$ and 16, and thus have

TABLE III. Excluded volume for polyethylene at 430 K. The columns titled A and B refer to calculations that use $d_m=3.9 \text{ \AA}$ ($\equiv d$), and $d_m=3.1656 \text{ \AA}$, respectively. The volume of the polyethylene molecule per site is estimated to be $0.28 d^3$.

| N | $v_e(N)/(Nd^3)$ | |
|-----|-------------------|-------------------|
| | A | B |
| 7 | 1.466 ± 0.016 | 1.164 ± 0.013 |
| 8 | 1.427 ± 0.016 | 1.138 ± 0.013 |
| 14 | 1.264 ± 0.007 | 1.025 ± 0.006 |
| 16 | 1.233 ± 0.009 | 1.003 ± 0.007 |
| 32 | 1.130 ± 0.009 | $.932 \pm 0.007$ |
| 48 | 1.092 ± 0.011 | $.905 \pm 0.009$ |
| 62 | 1.066 ± 0.009 | $.887 \pm 0.007$ |

$$v_e(N) = v_e(16) + (N-16) \frac{[v_e(16) - v_e(14)]}{2}. \quad (29)$$

We perform simulations of isolated RIS chains for chain lengths ranging from $N=7$ to 62. Independent chain configurations are generated by picking the torsional angles from the distribution given by the Flory weights. About 200–1000 independent configurations are generated for each chain length, and the volume and excluded volume are calculated via the method described for butane with $N_p=10^6$. The volume of a polyethylene molecule is estimated to be $0.28 Nd^3$ (from simulations), which results in a value of $d_m=3.1656 \text{ \AA}$. Simulation results for the excluded volume are summarized in Table III, and depicted in Fig. 2 [which is a plot of $v_e(N)/(Nd^3)$ vs $1/N$]. From the figure we can see that $v_e(N)/N$ is approximately linear in $1/N$ for $N \geq 14$. Also shown are the predictions of Eq. (29) (lines). The approximate expression represented by the lines is within the errors of the simulations for larger

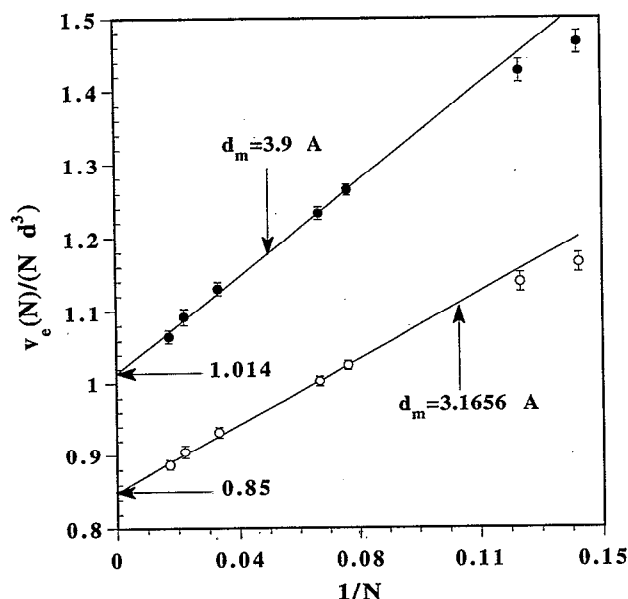


FIG. 2. Variation of the excluded volume of polyethylene ($T=430 \text{ K}$) with inverse degree of polymerization. Circles represent simulation results, lines represent predictions of Eq. (29).

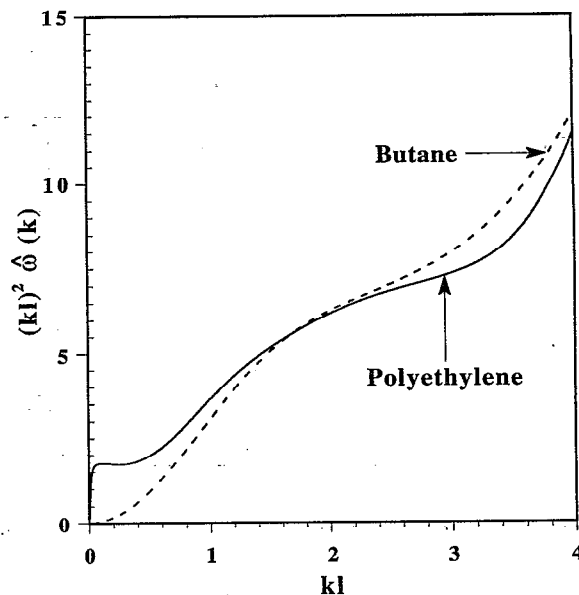


FIG. 3. Intramolecular structure factor of butane ($d=3.77 \text{ \AA}$, $T=300 \text{ K}$) and polyethylene ($N=6429$, $d=3.9 \text{ \AA}$, $T=430 \text{ K}$) plotted in standard Kratky form.

N , which gives us confidence in the extrapolation to large N . For polyethylene at 430 K ($d=3.9 \text{ \AA}$) the expressions for the excluded volumes are

$$\frac{v_e(N)}{d^3} = 17.70206 + 1.014(N-14), \quad (30)$$

for the GFD-A theory, and

$$\frac{v_e(N)}{d^3} = 14.349 + 0.85(N-14), \quad (31)$$

for the GFD-B theory. For $N=6429$, $Y_N/N=0.8278$ in the GFD-A theory and $Y_N/N=0.7724$ in the GFD-B theory.

V. RESULTS AND DISCUSSION

In this section we present results for the fluid structure (in the bulk and at a wall) and the equation of state of athermal butane and polyethylene. The results are for a temperature of 300 K for butane ($d=3.77 \text{ \AA}$, $l=1.53 \text{ \AA}$) and 430 K for polyethylene ($N=6429$, $d=3.9 \text{ \AA}$, $l=1.54 \text{ \AA}$).

A. Intramolecular and intermolecular correlations

Figure 3 compares the single chain structure factors of butane and polyethylene plotted in standard Kratky form. For large k , since this regime probes phenomena on length scales smaller than the size of the site, the single chain structure factors are qualitatively similar in butane and polyethylene. At small k , the polyethylene $(kl)^2 \hat{\omega}(k)$ shows a plateau which is not present in the butane curve. This plateau corresponds to the intermediate scaling regime, $lR_g^{-1} < kl < 1$ (where R_g is the radius of gyration) which is characteristic of ideal high polymer chains.

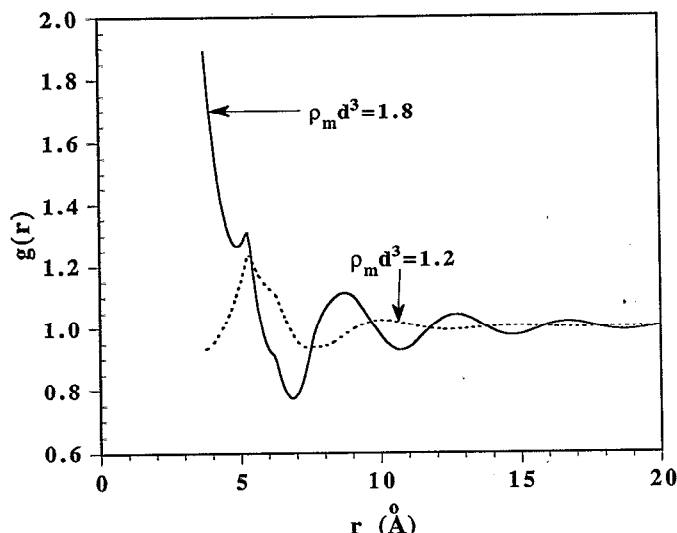


FIG. 4. Intermolecular site-site correlation functions, $g(r)$, in butane ($T=300$ K). The hard core diameter is 3.77 Å.

The intermolecular site-site correlation function, $g(r)$, in polymeric fluids is characterized by three regimes: at small r , $g(r)$ represents the local packing in the fluid which depends on the details of molecular geometry, at intermediate r , $g(r) - 1 = h(r)$ is negative due to the so-called correlation hole effect,^{18,29} and at large r ($r \gg R_g$), $g(r) = 1$. In small-molecule fluids, since R_g is of the order of the site size d , there is no qualitative separation of length scales between the hard-core diameter and the molecule size. Therefore, the correlation hole effect is not seen. Figures 4 and 5 depict the $g(r)$ of butane ($\rho_m d^3 = 1.2$ and 1.8) and polyethylene ($\rho_m d^3 = 1.8, 2.0$, and 2.2), respectively. Recall that the hard-core diameters are 3.77 and 3.9 Å for butane and polyethylene, respectively, so $g(r) = 0$ for smaller separations.

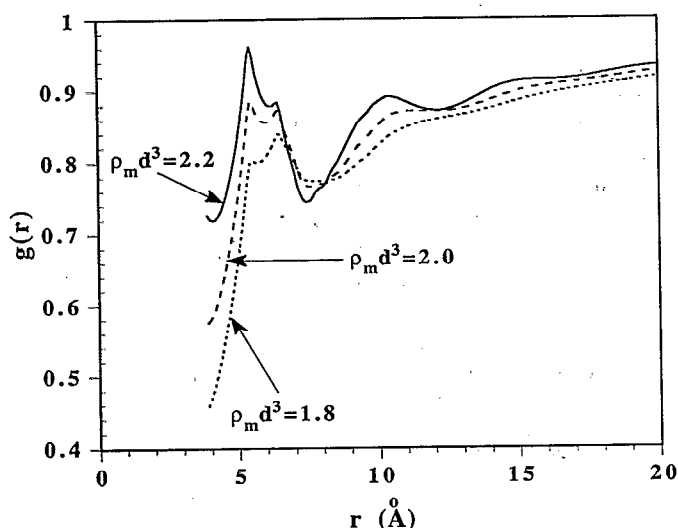


FIG. 5. Intermolecular site-site correlation functions, $g(r)$, in polyethylene ($N=6429$, $T=430$ K). The hard core diameter is 3.9 Å.

In polyethylene (Fig. 5) $g(r)$ near contact is less than one because configurational entropic restrictions on any given chain at short distances from another chain make a close approach unfavorable. This effect is most marked at the lowest density; as the density is increased the chains pack more efficiently, resulting in an increase in $g(d^+)$ with density. At the highest density, we see that solvation shells are beginning to form, and $g(r)$ is oscillatory for $r < 20$ Å. For small r one also sees various cusplike peaks in $g(r)$ [at $r=d$, $r=d+l$, and $r=d+l\sqrt{2(1-\cos\theta)}$] which are well-known consequences of the fixed bond lengths and bond angles employed in the molecular model.⁴⁹ For r greater than about 15 Å, $g(r)$ is a slowly increasing function of r . Here $g(r)$ is less than one because from any given site on a chain, sites on other polymers are excluded by the rest of the chain backbone. This correlation hole regime is important for r less than the size of the molecule. The shape of $g(r)$ is qualitatively similar at all the densities considered.

In butane (Fig. 4) entropic restrictions on the chains are not as severe as they are for polyethylene. At the lower density ($\rho_m d^3 = 1.2$) the $g(r)$ is qualitatively similar to that of polyethylene except that the correlation hole regime is absent (as expected). At the higher density ($\rho_m d^3 = 1.8$) $g(r)$ is sharply peaked near contact, and oscillatory for distances up to about 20 Å; well defined solvation shells can now be observed. The qualitative features of $g(r)$ in Fig. 4 have been previously observed.⁵⁰ The differences between $g(r)$ in butane and polyethylene arise from the much better packing and much weaker entropic restrictions in butane.

B. Wall-fluid correlations

Since the correlation hole effect is absent for collective density fluctuations, $g_w(z)$ at high densities has a (short) range of the order of the size of a *site*, in contrast to $g(r)$, which has a (long) range of the order of the size of a *molecule*. In small molecule fluids, $g(r)$ and $g_w(z)$ are qualitatively similar. Quantitative differences are present because the wall provides a much better surface for the molecules to pack against than does a single molecule.

These features are observed in Figs. 6 and 7 which compare $g_w(z)$ for butane ($\rho_m d^3 = 1.2$ and 1.8) and polyethylene ($\rho_m d^3 = 1.8, 2.0$, and 2.2), respectively. Recall that $z=0$ corresponds to the distance of closest approach of the sites to the wall, i.e., the wall (located at $z=0$) is impenetrable to the centers of the chain sites.

At meltlike densities, $g_w(z)$ is dominated by packing entropic effects;^{27,51} the chains tend to pile up against the wall because this is entropically more favorable. A smooth structureless wall provides a favorable surface against which the chains can pack. Therefore, $g_w(z)$ is greater than 1 (for small z) in all the curves in Figs. 6 and 7. As was the case for $g(r)$, there are cusplike peaks at short distances due to the fixed bond lengths and bond angles. In all the cases (even for butane at the lower density), $g_w(z)$ is an oscillatory function of z with a period of about a site diameter: this is evidence for the layering of the chains at the

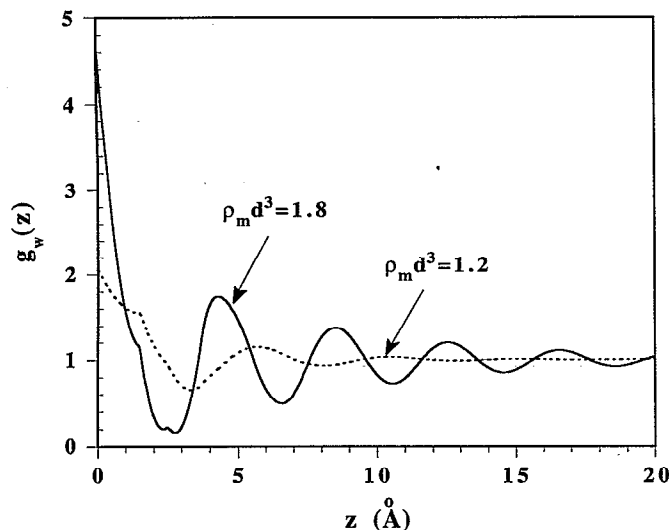


FIG. 6. Wall-fluid correlation function in butane under the same conditions as in Fig. 4. The wall is impenetrable to the centers of the sites and is located at $z=0$. The density profile may be obtained by multiplying $g_w(z)$ by the density.

surface. The oscillations in $g_w(z)$ are more pronounced than those in $g(r)$ because the wall is a much stronger nonuniformity than a single bead. As mentioned earlier, $g_w(z)$ also has a short range. In fact, even at the highest density for polyethylene, $g_w(z)$ appears to have decayed to 1 within about $z \approx 20$ Å (about five site diameters). The enhancement of the chain density near the wall, characterized by the value of $g_w(0)$, is much higher for butane than it is for polyethylene because the configurational entropic restrictions near the wall on a single butane molecule are much less important than those for a single polyethylene

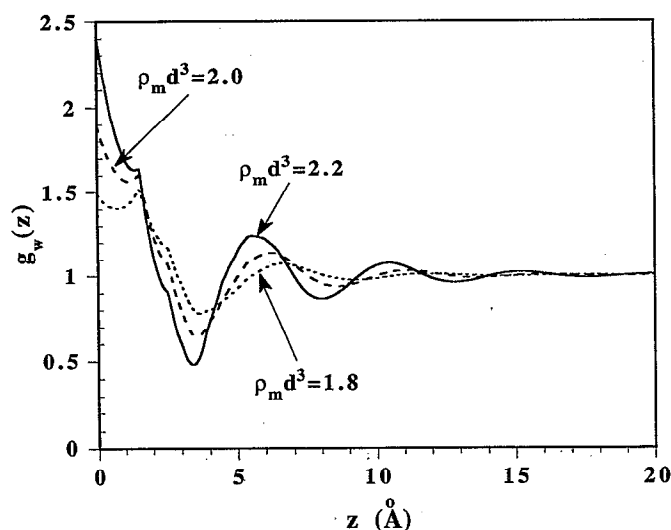


FIG. 7. Wall-fluid correlation function in polyethylene under the same conditions as in Fig. 5. The wall is impenetrable to the centers of the sites and is located at $z=0$. The density profile may be obtained by multiplying $g_w(z)$ by the density.

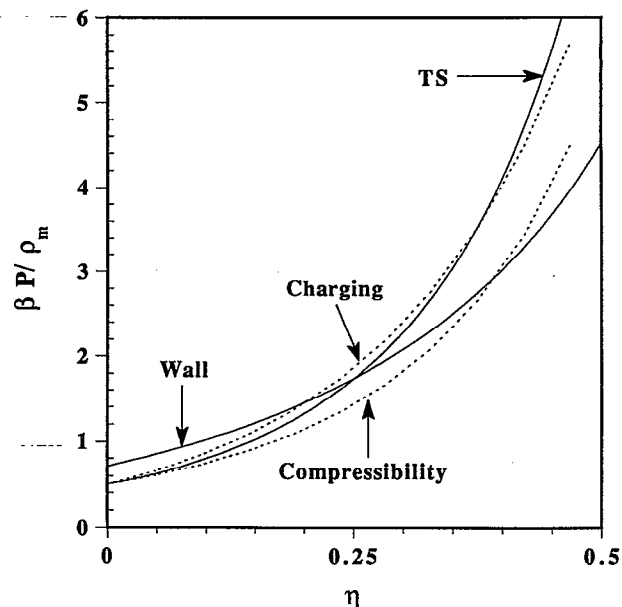


FIG. 8. Comparison of the various theories (as marked) for the equation of state of hard diatomics ($l/d=0.6$). The Tildesley-Streett (TS) equation is a fit to simulation data (Ref. 47). For hard diatomics, the GFD theories reduce to the TS equation.

molecule. Therefore, the butane molecules can pack more efficiently at the wall. This also causes the more severe oscillations in $g_w(z)$ in butane at the higher density, where several layers of adsorbed molecules are observed.

C. Equation of state

Figures 8, 9, and 10 compare the hard chain contributions to the pressure predicted by the various theories for diatomics ($l/d=0.6$), butane ($l=1.53$ Å, $d=3.77$ Å, $T=300$ K), and polyethylene ($l=1.54$ Å, $d=3.9$ Å, $T=430$ K), respectively.

Figure 8 compares the wall, charging, and compressibility equations of state to the Tildesley-Streett (TS)⁴⁷ equation (which is a fit to simulation data; the GFD theories reduce to the TS equation of state⁴⁷ for diatomics.) The compressibility pressure is always lower than the TS pressure, which is not surprising, and consistent with earlier observations on short flexible chains.¹¹ The charging and wall routes tend to overestimate the pressure at low densities, and underestimate the pressure at high densities. The behavior of the wall theory is similar to what has been reported in studies of short flexible chains.²⁶ The charging route is in very good agreement with the TS equation over the entire range of densities investigated. With the exception of the wall route, all the equations are exact in the low density limit, i.e., $Z \rightarrow 1$ as $\rho \rightarrow 0$.

The relative predictions of the various theories are similar for butane and polyethylene, except that the spread between the charging and the compressibility pressures increases with N . Figure 9 depicts the predictions of the various theories for the pressure of butane. The GFD-A theory is virtually indistinguishable from the GFD-B the-

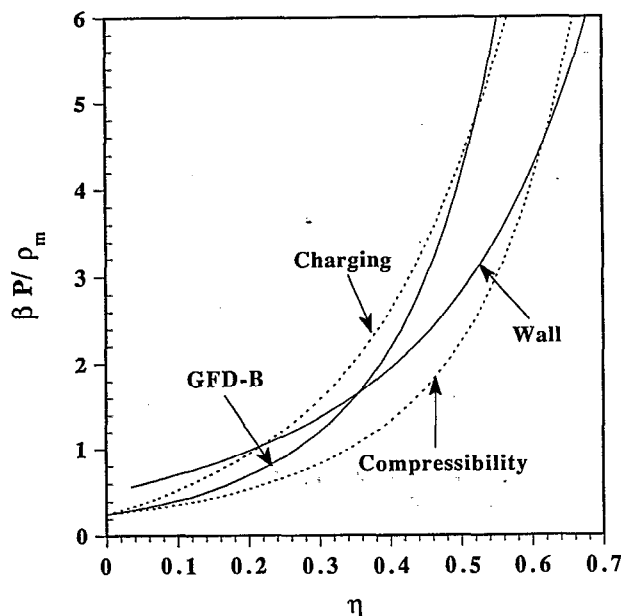


FIG. 9. Comparison of the various theories (as marked) for the equation of state of hard core butane ($T=300$ K).

ory and is therefore not shown. We note that the GFD-A theory has been shown to be very accurate for triatomics,⁵ and therefore expect both the GFD approaches to be accurate for butane also. Unfortunately, since simulation data for athermal alkanes are not available, it is not possible to unambiguously determine which theory is the most accurate. Therefore, we resort to a relative comparison to determine which theory is most likely to be accurate. The relative behavior is qualitatively similar to what is observed for diatomics if we replace the TS equation with the GFD-B theory. Therefore it is tempting to speculate that the GFD-B theory is the most accurate, with the charging predictions being too high and the compressibility predictions being too low.

The results for polyethylene are presented in Fig. 10 and are qualitatively similar to those for butane although there are two differences. First, the spread between the charging and compressibility pressure is now very large, which reflects an interesting decrease in the thermodynamic consistency of the PRISM theory as N increases. Second, the charging route pressure remains greater than the GFD predictions up to very high packing fractions. Also shown in Fig. 10 is the GFD-A equation of state, which results in pressures that are significantly lower than the GFD-B theory for all densities.

VI. CONCLUSIONS

In this paper, we have investigated the athermal contribution to the pressure of polyethylene and butane. A realistic molecular model is chosen, the parameters of which are either obtained from the literature, or from matching theoretical predictions for the structure factor to wide angle scattering experiments. Various theories for the pressure have been studied: two via extensions of mean-

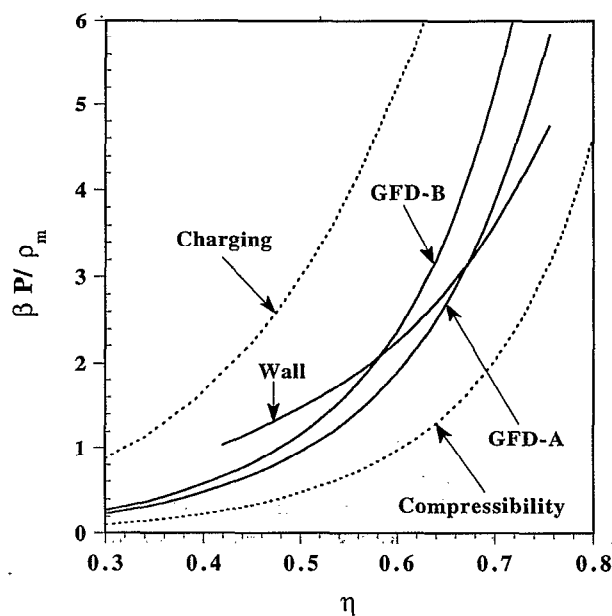


FIG. 10. Comparison of the various theories (as marked) for the equation of state for hard-core polyethylene ($N=6429$).

field generalized Flory ideas, and three via different thermodynamic routes in the PRISM theory. It is found that the uncertainty in the hard-chain pressure increases with increasing chain length: the various theories are in fair agreement for diatomics, but the spread between the theories becomes large for polyethylene. The relative predictions of the theories appear to be largely independent of chain length, however, and from the behavior for diatomics (where simulation data is available) we speculate that one of the mean field theories (GFD-B) is probably the most accurate. Of the integral equation routes investigated, the wall-PRISM predictions appear to be the best at the liquid densities of interest since it lies between the charging and compressibility pressures. The charging route overestimates the pressure and the compressibility route underestimates the pressure.

One problem with obtaining equations of state from realistic molecular models *without* fitting the parameters to thermodynamic data is that the potential parameters are generally difficult to obtain. Computer simulations are therefore useful because they allow a test of the molecular model without the approximations that theoretical treatments necessarily entail. However, there seems to be some disagreement in the literature regarding the appropriate potential parameters for the alkanes. For alkane models where all the sites are considered to be identical, Lopez-Rodriguez *et al.*³¹ found that the potential parameters were a function of the chain length, i.e., end effects were important. Ryckaert and Bellemans³⁰ found the opposite, i.e., that the same parameters gave good results for butane and octane. To add to the confusion, while Dodd and Theodorou⁵² find good agreement (for the pressure) between their simulations (using the Ryckaert-Bellemans parameters) and experiments on polyethylene, the simulations of

Boyd¹⁰ using similar parameters predict (unphysical) negative pressures!

In the study of nonpolar liquids, one generally treats the repulsive potential and the attractive potential using different approaches. For dense fluids, the thermodynamic consequences of the attractive forces can generally be accurately determined by perturbation methods. It is therefore of interest to be able to test each of these aspects of the theory independently. For this reason, it would be very useful to have available simulation results for athermal alkanes in order to effectively discriminate between various hard-chain theories.

ACKNOWLEDGMENTS

Work at Illinois was sponsored by the Division of Materials Sciences, Office of Basis Energy Sciences, U.S. Department of Energy. Work at Sandia National Laboratories was supported by the U.S. Department of Energy under Contract No. DE-AC0476DP00789. A. Y. thanks Professor Carol K. Hall for useful discussions and permission to use computer programs developed by him while he was at North Carolina State University.

- ¹A. Firoozabadi, *J. Pet. Technol.* **40**, 297 (1988); K. C. Chao and R. L. Robinson, *Equations of State: Theories and Applications* (American Chemical Society, Washington, D.C., 1987).
- ²P. J. Flory, *J. Chem. Phys.* **10**, 51 (1942); M. L. Huggins, *Ann. N. Y. Acad. Sci.* **43**, 1 (1942); E. A. Guggenheim, *Proc. R. Soc. London, Ser. A* **203**, 203 (1944); R. Simha and T. Somcynsky, *Macromolecules* **2**, 342 (1969); I. C. Sanchez and R. H. Lacombe, *J. Phys. Chem.* **80**, 2352, 2568 (1976); *Macromolecules* **11**, 1145 (1978); *J. Phys. Chem.* **80**, 2352, 2568 (1976); *Macromolecules* **11**, 1145 (1978); M. G. Bawendi and K. F. Freed, *J. Chem. Phys.* **88**, 2741 (1988); J. Dudowicz, K. F. Freed, and W. G. Madden, *Macromolecules* **23**, 1181 (1990); J. E. G. Lipson and S. S. Andrews, *J. Chem. Phys.* **96**, 1426 (1992).
- ³I. Prigogine, *The Molecular Theory of Solutions* (North-Holland, Amsterdam, 1957); S. Beret and J. M. Prausnitz, *Macromolecules* **8**, 878 (1975); M. D. Donohue and J. M. Prausnitz, *AIChE J.* **24**, 848 (1978).
- ⁴R. Dickman and C. K. Hall, *J. Chem. Phys.* **85**, 4108 (1986).
- ⁵K. G. Honnell and C. K. Hall, *J. Chem. Phys.* **90**, 1841 (1989).
- ⁶A. Yethiraj and C. K. Hall, *J. Chem. Phys.* **95**, 8494 (1991).
- ⁷A. Yethiraj and C. K. Hall, *J. Chem. Phys.* **95**, 1999 (1991).
- ⁸M. S. Wertheim, *J. Chem. Phys.* **87**, 7323 (1987); W. G. Chapman, G. Jackson, and K. E. Gubbins, *Mol. Phys.* **65**, 1057 (1988); Y. C. Chiew, *Mol. Phys.* **70**, 129 (1990); T. Boublík, C. Vega, and M. Diaz-Pena, *J. Chem. Phys.* **93**, 730 (1990).
- ⁹M. Bishop, D. Ceperley, H. L. Frisch, and M. H. Kalos, *J. Chem. Phys.* **72**, 3228 (1980); D. J. Rigby and R. J. Roe, *ibid.* **88**, 5280 (1988); D. Brown and J. H. R. Clarke, *ibid.* **92**, 3062 (1990); S. Toxvaerd, *ibid.* **93**, 4290 (1990); K. Mansfield and D. N. Theodorou, *Macromolecules* **24**, 4295 and 6283 (1991); N. G. Almaraz, E. Enciso, and F. J. Bernejo, *J. Chem. Phys.* **96**, 4625 (1992).
- ¹⁰R. H. Boyd, *Macromolecules* **22**, 2477 (1989).
- ¹¹K. S. Schweizer and J. G. Curro, *J. Chem. Phys.* **89**, 3342 (1988); **89**, 3350 (1988).
- ¹²J. A. Barker and D. Henderson, *J. Chem. Phys.* **47**, 4714 (1967).
- ¹³J. G. Curro, A. Yethiraj, K. S. Schweizer, and J. D. McCoy, *Macromolecules* (submitted).
- ¹⁴J. G. Curro and K. S. Schweizer, *J. Chem. Phys.* **87**, 1842 (1987).
- ¹⁵D. Chandler, and H. C. Andersen, *J. Chem. Phys.* **57**, 1930 (1972).
- ¹⁶D. Chandler, *J. Chem. Phys.* **59**, 2742 (1973).
- ¹⁷D. Chandler, in *Studies in Statistical Mechanics VIII* (North-Holland, Amsterdam, 1982), p. 275, and references cited therein.
- ¹⁸K. S. Schweizer and J. G. Curro, *Phys. Rev. Lett.* **58**, 256 (1987); J. G. Curro and K. S. Schweizer, *Macromolecules* **20**, 1928 (1987).
- ¹⁹A. Yethiraj, C. K. Hall, and K. G. Honnell, *J. Chem. Phys.* **93**, 4453 (1990).
- ²⁰A. Yethiraj and C. K. Hall, *J. Chem. Phys.* **96**, 797 (1992).
- ²¹J. G. Curro, K. S. Schweizer, G. S. Grest, and K. Kremer, *J. Chem. Phys.* **91**, 1357 (1989).
- ²²K. G. Honnell, J. D. McCoy, J. G. Curro, K. S. Schweizer, A. H. Narten, and A. Habenschuss, *J. Chem. Phys.* **94**, 4659 (1991); A. Narten, A. Habenschuss, K. G. Honnell, J. D. McCoy, J. G. Curro, and K. S. Schweizer, *Discuss. Faraday Soc.* **88**, 1791 (1992).
- ²³J. D. McCoy, K. G. Honnell, K. S. Schweizer, and J. G. Curro, *Chem. Phys. Lett.* **179**, 374 (1991); *J. Chem. Phys.* **95**, 9348 (1991).
- ²⁴K. G. Honnell, C. K. Hall, and R. Dickman, *J. Chem. Phys.* **87**, 664 (1987).
- ²⁵J. Gao and J. H. Weiner, *J. Chem. Phys.* **91**, 3168 (1989).
- ²⁶A. Yethiraj and C. K. Hall, *J. Chem. Phys.* **95**, 3749 (1991).
- ²⁷R. Dickman and C. K. Hall, *J. Chem. Phys.* **89**, 3168 (1988).
- ²⁸M. V. Volkenstein, *Configurational Statistics of Polymeric Chains* (Interscience, New York, 1963); P. J. Flory, *Statistical Mechanics of Chain Molecules* (Wiley, New York, 1969).
- ²⁹P. J. Flory, *J. Chem. Phys.* **17**, 303 (1949); P. J. Flory, *Principles of Polymer Chemistry* (Cornell University, Ithaca, 1953); P.-G. deGennes, *Scaling Concepts in Polymer Physics* (Cornell University, Ithaca, 1979).
- ³⁰J. P. Ryckaert and A. Bellemans, *Chem. Phys. Lett.* **30**, 123 (1975); *Faraday Discuss. Chem. Soc.* **66**, 95 (1978).
- ³¹A. Lopez Rodriguez, C. Vega, J. J. Freire, and S. Lago, *Mol. Phys.* **73**, 691 (1991); A. Lopez Rodriguez and J. J. Freire, *ibid.* **63**, 591 (1988).
- ³²W. G. Madden and S. A. Rice, *J. Chem. Phys.* **72**, 4208 (1980).
- ³³A. H. Narten, E. Johnson, and A. Habenschuss, *J. Chem. Phys.* **73**, 1248 (1980); A. H. Narten and A. Habenschuss, *J. Chem. Phys.* **75**, 3073 (1981).
- ³⁴A. Yethiraj and K. S. Schweizer, *J. Chem. Phys.* **97**, 5927 (1992).
- ³⁵There are discrepancies between theory and experiment for large k which have been attributed entirely to bond and angle vibrations which are absent in this model. The agreement with experiment becomes quantitative at large k when these thermal oscillations are accounted for (Ref. 22). Since the model potential does not include any attractive component, it is not expected to accurately describe the $k \rightarrow 0$ behavior since this is a thermodynamic quantity. In addition, the diffraction experiments at very small k are inaccurate due to parasitic scattering effects.
- ³⁶G. L. Slonimskii, A. A. Askadskii, and A. I. Kitaigorodskii, *Polym. Sci. USSR* **12**, 556 (1970).
- ³⁷J. D. McCoy, K. G. Honnell, J. G. Curro, K. S. Schweizer, and A. H. Narten (in preparation).
- ³⁸K. S. Schweizer, K. G. Honnell, and J. G. Curro, *J. Chem. Phys.* **96**, 3211 (1992); J. M. Melenkevitz, J. G. Curro, and K. S. Schweizer (in preparation).
- ³⁹J. D. McCoy, K. G. Honnell, J. G. Curro, K. S. Schweizer, and J. D. Honnecutt, *Macromolecules* **25**, 4905 (1992).
- ⁴⁰A. Yethiraj and K. S. Schweizer, *J. Chem. Phys.* **97**, 1455 (1992).
- ⁴¹L. J. Lowden and D. Chandler, *J. Chem. Phys.* **59**, 6587 (1973); **62**, 4246 (1975).
- ⁴²J.-P. Hansen and I. R. McDonald, *Theory of Simple Liquids* (Academic, San Diego, 1986).
- ⁴³D. Henderson, F. F. Abraham, and J. A. Barker, *Mol. Phys.* **31**, 1291 (1975).
- ⁴⁴Y. Zhou and G. Stell, *Mol. Phys.* **66**, 767 (1989).
- ⁴⁵A. Yethiraj and C. K. Hall, *J. Chem. Phys.* **94**, 3943 (1991).
- ⁴⁶N. F. Carnahan and K. E. Starling, *J. Chem. Phys.* **51**, 635 (1969).
- ⁴⁷D. J. Tildesley and W. B. Streett, *Mol. Phys.* **41**, 341 (1980).
- ⁴⁸J. Alejandre and G. A. Chapela, *Mol. Phys.* **61**, 1119 (1987); M. Denlinger and C. K. Hall, *ibid.* **71**, 541 (1990).
- ⁴⁹B. M. Ladanyi and D. Chandler, *J. Chem. Phys.* **62**, 4308 (1975).
- ⁵⁰C. S. Hsu, L. R. Pratt, and D. Chandler, *J. Chem. Phys.* **68**, 4213 (1978); J. R. Elliott and U. S. Kanetkar, *Mol. Phys.* **71**, 871 (1990).
- ⁵¹A. Yethiraj and C. K. Hall, *J. Chem. Phys.* **91**, 4827 (1989); *Macromolecules* **23**, 1865 (1990).
- ⁵²L. R. Dodd and D. N. Theodorou, *Polymer Prep.* **33**, 645 (1992).